

Density of states of amorphous In-Ga-Zn-O from electrical and optical characterization

Eric Kai-Hsiang Yu,¹ Sungwoo Jun,² Dae Hwan Kim,² and Jerzy Kanicki^{1,a)}

¹Department of Electrical Engineering and Computer Science, University of Michigan, Ann Arbor, Michigan 48109, USA

²School of Electrical Engineering, Kookmin University, 861-1 Jeongneung-dong, Seongbuk-gu, Seoul 136-702, South Korea

(Received 25 July 2014; accepted 5 October 2014; published online 17 October 2014)

We have developed a subgap density of states (DOS) model of amorphous In-Ga-Zn-O (a-IGZO) based on optical and electrical measurements. We study the optical absorption spectrum of the a-IGZO using UV-Vis spectroscopy. Together with the first-principles calculations and transient photoconductance spectroscopy from the literature, we determine that the valence band tail and deep-gap states are donors and can be described by exponential and Gaussian distributions, respectively. The conduction band tail and deep-gap states are examined using multi-frequency capacitance-voltage spectroscopy on a-IGZO thin-film transistors (TFTs). The extracted conduction band DOS are fitted to exponential (bandtail) and Gaussian (deep-gap) functions and their validity are supported by the activation energy vs. gate-source bias relationship of the a-IGZO TFT. The PL deep-level emission, which is almost identical to the conduction band deep-gap Gaussian, suggests that these states should be assigned as acceptors. The donor/acceptor assignments of subgap states are consistent with the 2D numerical TFT simulations. © 2014 AIP Publishing LLC.

[<http://dx.doi.org/10.1063/1.4898567>]

I. INTRODUCTION

In amorphous semiconductors, localized states within the band gap arise from structural disorder (bond angles and length variations), dangling bonds, non-stoichiometry, and carrier scattering at defect sites.^{1,2} Such sub-gap density of states (DOS) dominates the electrical properties and stability of thin-film transistors (TFTs). A DOS model is needed to thoroughly understand and optimize TFT electrical properties and stability. The DOS is also required for the design of devices and circuits using 2D numerical and SPICE simulations, respectively. To realize the mass-production of next-generation ultra-high definition amorphous In-Ga-Zn-O (a-IGZO)-backplane active-matrix flat-panel display, a robust a-IGZO DOS model is very desirable.

To date, the topic of a-IGZO DOS has been the focus of much rigorous debate and discussion in peer-reviewed literature. Hsieh *et al.* extracted the density of acceptor-like states near the conduction band minimum (E_C) in a-IGZO by fitting TFT current-voltage (I - V) data to TCAD simulations originally developed for hydrogenated amorphous silicon (a-Si:H) technology.³ Nomura *et al.* observed a large density of subgap states near the valence band maximum (E_V), possibly the origin for the lack of p -type operation, using hard x-ray photoelectron spectroscopy.⁴ Below the band gap, optical absorption spectrum showed tail-like decay that can be described by the Urbach relation, although its characteristic energy slope in the literature varies with sample quality and preparation.⁴⁻⁶ Kamiya *et al.* and Chen *et al.* performed first-principles calculations using density functional theory and

found that for IGZO, oxygen vacancies form fully occupied donor levels located at ~ 1 eV above E_V .^{5,7} Temperature-dependent TFT characteristics can also be used to extract DOS near the E_C , as shown by Chen *et al.* with the Meyer-Neldel rule⁸ and Lee and Nathan with trap-limited conduction at low-temperature (77 K).⁹ Capacitance-voltage (C - V) measurement can reliably probe the density of defect states in a semiconductor device and is commonly used in silicon CMOS technology. From the C - V measurements of an a-IGZO TFT structure, Kimura *et al.* extracted the DOS near the E_C .¹⁰ In the case of TFTs with non-negligible bulk resistivity, the frequency of the AC small-signal needs to be very low (< 1 Hz) so the electrons supplied from the source/drain regions can have sufficient time to respond. Extraction of the DOS from high-frequency C - V measurements is demonstrated by Jeon *et al.*, who exposed a-IGZO TFT to monochromatic sub-band gap light acting as a source of photo-excitation.¹¹ Considering that a-IGZO is sensitive to bias-illumination degradation, the measurement should be done without exposure to light. Lee *et al.* developed an a-IGZO TFT capacitance model that allows for the frequency-independent capacitance of localized states, and in turn the acceptor-like DOS, to be derived using the multi-frequency C - V response without illumination.¹² However, none of these works have addressed the need for a comprehensive a-IGZO sub-gap DOS model that is robust enough to accommodate a wide variety of deposition conditions and has explicitly defined acceptor/donor assignments derived from experimental and theoretical evidence.

In this paper, using a combination of optical methods and C - V measurements that are described in the literature, we develop an a-IGZO DOS model over the entire range of the band-gap. We also incorporate published data in the

^{a)}Author to whom correspondence should be addressed. Electronic mail: kanicki@eecs.umich.edu.

literature to complement and calibrate our experimental results. The photoluminescence (PL) spectrum, though commonly used in the analysis of compound (III-V, II-VI) semiconductors, is rarely reported for a-IGZO.^{13–15} We measure the PL spectrum of a-IGZO thin film to confirm the results of our DOS extraction and, together with numerical simulations, assist the assignment of sub-gap states as either donor or acceptor-like. By building our a-IGZO DOS model from multiple sources, we expect it to be robust and applicable to any laboratory research or industrial production setting.

II. EXPERIMENT

An a-IGZO thin film with thickness of 100 nm is deposited using rf sputtering at room temperature on a clean quartz glass substrate. The sample is then annealed at 300 °C for 30 min in ambient air on a hot plate. The optical absorption spectrum of the a-IGZO thin film is measured with a Cary 5E UV-Vis spectrometer. The spectrometer collects the thin-film transmittance of a polarized monochromatic light with wavelength varying from 300 nm (4 eV) to 1000 nm (1.24 eV). The PL spectrum of the a-IGZO film is then measured at $T = 300$ K and at $T = 8$ K using a system consisting of a grating monochromator, lock-in amplification, a photodiode detector, and a closed-cycle helium cryostat. The source of the PL excitation is a He-Cd laser of wavelength $\lambda = 325$ nm with laser power of 50 W/cm². An in-house LabView program adjusts the monochromator during data collection to sweep the emission wavelength from 330 nm to 700 nm at 1 nm intervals with 300 ms integration time.

For the a-IGZO TFT multi-frequency C - V measurements, bottom-gate TFTs are fabricated on glass substrates. The gate metal is first sputtered, defined, and then followed by a bilayer of PECVD gate insulator. The gate insulator is a 400-nm layer of a-SiN_x (interfacing with gate metal) and 50-nm layer a-SiO_x (interfacing with the a-IGZO). The 45 nm-thick a-IGZO islands are sputtered, defined, and followed by the source/drain electrodes. The fabricated devices have width (W) = 25 μ m and length (L) = 10 μ m. The C - V characteristics between the gate and source/drain (tied together) electrodes are measured for six different a-IGZO TFTs on the same substrate by using an LCR meter (HP 4284 A) at room temperature in the dark. The gate-to-source/drain voltage ($V_{G-S/D}$) range is from -20 to 20 V, and its ramp-up speed is 0.4 V/s. The amplitude (A) and frequencies (f_n) of the small-signal voltage used are $A = 0.05$ V and $f_1 = 50$ kHz, $f_2 = 250$ kHz, and $f_3 = 1$ MHz. With one of the six a-IGZO TFTs, we also measured the temperature-dependent I - V characteristics from 30 °C to 70 °C (10 °C intervals) and extracted the drain current activation energy⁸ (E_{act}) as a function of the gate-to-source voltage (V_{GS}) under a fixed drain-to-source voltage (V_{DS}) = 0.1 V.

III. RESULTS AND DISCUSSION

The optical absorption spectrum (α) of the a-IGZO thin film on a quartz substrate is shown in linear and semi-logarithmic scale in Fig. 1(a). For incident photon energies greater than 3 eV, a-IGZO shows strong absorption of at least 10^4 cm⁻¹ and α increases linearly with energy. The optical

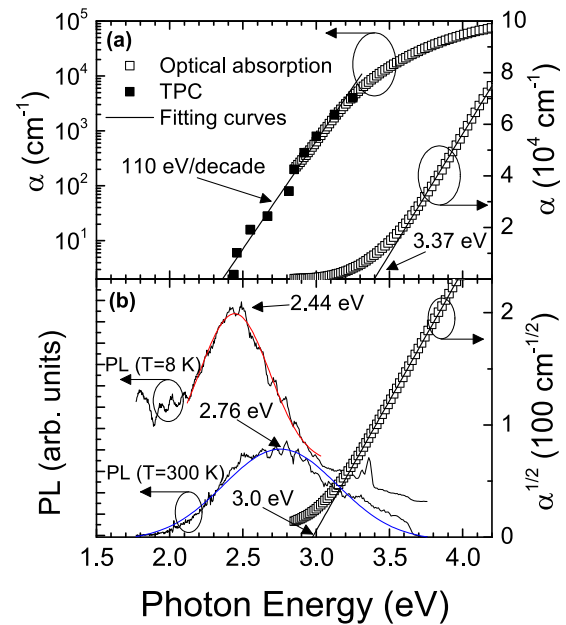


FIG. 1. (a) The absorption spectrum of a-IGZO thin film is shown in linear and semi-logarithmic scale as empty squares (\square). The transient photocapacitance (TPC) spectroscopy data from literature¹⁷ are reproduced in the figure as solid squares (\blacksquare). The absorption edge in linear scale is used to extract the optical gap by extrapolating the x-intercept. (b) The PL emission at $T = 8$ K and $T = 300$ K are shown and fitted to Gaussian functions. The Tauc gap energy is extracted from the square root of optical absorption.

band gap $E_g = 3.37$ eV can be extracted from α by extrapolating the absorption edge to its x-intercept. In the semi-logarithmic scale of Fig. 1(a), the exponential decay of α , or the Urbach edge, is visible for energies below E_g . It can be described by the equation

$$\alpha(\hbar\omega) = \alpha_0 \exp\left(\frac{E - \hbar\omega}{E_0}\right), \quad (1)$$

where E_0 is the characteristic energy slope of the Urbach edge and α_0 is a constant factor. The Urbach edge, which was first reported for alkali halide crystals,¹⁶ represents the band broadening due to disorder and is observed in all amorphous semiconductors.¹ In the figure, α is truncated at 2.81 eV, after which the signal intensity falls below the detection background of the UV-Vis spectrometer. More data points are required to precisely determine the slope of the Urbach edge and extract E_0 . To achieve this, the transient photocapacitance (TPC) spectroscopy data of the a-IGZO metal-insulator-semiconductor (MIS) structure is adapted from Erslev¹⁷ and reproduced in Fig. 1(a) as solid squares. Details regarding TPC spectroscopy can be found elsewhere^{18,19} and is summarized here. A voltage filling pulse (zero bias) is first applied to the reverse-biased MIS junction to fill the previously depleted regions. Immediately after the voltage pulse, the capacitance transient is measured while a sub-band gap light is illuminating the sample. These two steps are then repeated minus the optical excitation. The measured transient signals are each integrated over the time between the two pulses, and their difference, normalized over photon flux, is taken to be the TPC at that photon energy. Repeating this process for photon energies of interest

produces the TPC spectrum. At low optical intensities, the TPC signal is proportional to the joint DOS, similar to optical absorption but at much greater sensitivity.¹⁸ Therefore, the signal decay in TPC spectrum is also the Urbach edge. Since we are only interested in the slope instead of actual values, the TPC data, which is in arbitrary units vs. photon energy, can be calibrated to Fig. 1(a) by vertically aligning its data points (solid squares) with absorption (open squares) at corresponding energy values until the two curves effectively overlap over a significant range of values. We then extract the characteristic Urbach energy to be $E_0 = 110.5 \pm 2.3$ meV. Assuming parabolic band edges, the Tauc gap energy of 3.0 eV can also be extrapolated from $\sqrt{\alpha}(E)$ as shown in Fig. 1(b). This value is consistent with our previous work⁶ and other reported values in the literature.^{4,5}

The PL spectrum of thin-film a-IGZO at $T = 8$ K and $T = 300$ K are shown in Fig. 1(b) for emissions between 330 nm (3.75 eV) and 700 nm (1.77 eV). At $T = 8$ K, we observe a broad deep-level emission at 2.44 eV followed by a weak near band-edge (NBE) emission at 3.4 eV. At room temperature, the NBE emission is almost completely obscured. We fit the deep-level emission with a Gaussian function and find that at $T = 300$ K the emission is centered at $\lambda = 2.76$ eV with full-width at half-maximum (FWHM) of $\Delta E_{1/2} = 0.91$ eV. At $T = 8$ K, the deep-level emission is described by $\lambda = 2.44$ eV and $\Delta E_{1/2} = 0.57$ eV. In PL spectroscopy, after an electron has been excited to the conduction band, there are four possible recombination processes: (i) band-to-band, (ii) electron trap-to-hole trap, (iii) band-to-hole trap, and (iv) electron trap-to-band. In the PL spectrum, the dominance of the deep-level emission over the NBE emission is similar to what was reported in the literature,^{13,15} meaning that the main radiative recombination process in a-IGZO cannot be band-to-band transition and must involve at least a trap level. We note that the deep-level emission peak energies are different from the one detected near 1.77 eV (700 nm) by Yamaguchi *et al.* At $T = 8$ K in Fig. 1(b), there appears to be a small PL response at 1.77 eV in our a-IGZO thin film, but because it is at the edge of our detection range, we limit our discussion to the peak at 2.76 eV within the scope of this work. We speculate that the peaks represent two distinct transitions within the band gap, and both or only one may be observed prominently in a-IGZO depending on deposition conditions and measurement setup.

We extract the DOS near E_C using multi-frequency C - V spectroscopy,¹² which is briefly described as follows. As shown in Fig. 2 inset (i), the a-IGZO TFT under test can be modeled with an equivalent circuit of: gate insulator capacitance (C_{OX}), capacitance of V_{GS} -responsive charges captured/released by the subgap states at corresponding energy levels (C_{LOC}), equivalent resistance of the C_{LOC} -related charges (R_{LOC}), and capacitance of V_{GS} -responsive free carriers (C_{FREE}). Assuming that the f -dependence is entirely contained in the channel-to-S/D series resistance (R_S), the f -independent intrinsic C - V can be derived from the C - V at different frequencies. The C - V at $f = 50$ kHz, 250 kHz, and 1 MHz for a single TFT are shown in Fig. 2 inset (ii). From the resulting f -independent C - V (not shown), we can extract

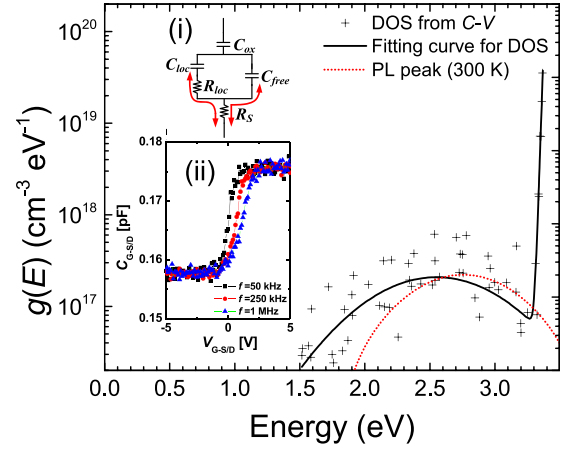


FIG. 2. The a-IGZO DOS extracted from multi-frequency C - V measurements (crosshairs, +) and the associated fitting curve. Inset (i) shows the equivalent RC model used to extract the DOS from multi-frequency C - V measurements of a-IGZO TFTs. Inset (ii) shows the frequency-dependent C - V for one of the six a-IGZO TFTs as measured.

the DOS located in the range of energies observable by electrical measurements. This is repeated for six different TFTs on the same substrate and the combined DOS are shown in Fig. 2 as crosshairs (some points omitted for clarity). We observe in Fig. 2 that at energies closer to E_C , the bandtail states are an exponential distribution and can be described by the equation

$$g_{ta}(E) = N_{ta} \exp\left(\frac{E - E_C}{E_a}\right), \quad (2)$$

where N_{ta} is the maximum density of the conduction bandtail states and E_a is the bandtail slope. We then extract $N_{ta} = 4.2 \times 10^{19} \text{ eV}^{-1} \text{ cm}^{-3}$ and $E_a = 11 \pm 0.3$ meV by fitting the data points to (2). The conduction bandtail slope extracted this way is comparable to the values derived from numerical simulation²⁰ and carrier transport²¹ studies. The deep-gap states we model using a Gaussian distribution of the form

$$g_{ga}(E) = N_{ga} \exp\left[-\left(\frac{E - \lambda_a}{\sigma_a}\right)^2\right], \quad (3)$$

where N_{ga} , λ_a , and σ_a are the Gaussian peak value, the mean energy, and the standard deviation, respectively. We calculate the parameters $N_{ga} = 2 \times 10^{17} \text{ eV}^{-1} \text{ cm}^{-3}$, $\lambda_a = 2.55 \pm 0.37$ eV, and $\sigma_a = 0.69$ eV by fitting the DOS near the midgap to (3). The λ_a and the FWHM ($\Delta E_{1/2} = 0.97$ eV) of the E_C deep-gap states are very close to those of the PL deep-level emission observed in Fig. 1(b). To verify this visually, we superimpose a Gaussian distribution centered at $\lambda = 2.76$ eV representing the PL deep-level emission in Fig. 2 as a dashed curve. We observe a significant overlap of the two Gaussians, which suggests that they are possibly of the same origin involving deep-gap states near the E_C .

To validate the DOS extracted from multi-frequency C - V , E_{act} as a function of V_{GS} is extracted from the temperature-dependent I - V characteristics from 30 °C to 70 °C following the methodology described in Chen *et al.*⁸

The Arrhenius plot and the extracted E_{act} as a function of V_{GS} are shown in Figs. 3(a) and 3(b), respectively. The E_{act} in the figure is the average barrier height for an electron trapped in the localized states to jump into the conduction band. It represents the difference between the E_{C} and the Fermi level at the a-IGZO/gate insulator interface ($E_{\text{C}} - E_{\text{F}}$) and any influences from the bulk. It has been shown in a-Si:H TFT numerical simulations that at high V_{GS} , the deep-gap states have no influence on E_{act} , which actually approaches E_{a} for values less than 20 meV.²² Assuming a sharp conduction bandtail slope, the movement of E_{F} in response to V_{GS} would become limited in the vicinity of a large density of tail states, i.e., when E_{act} approaches E_{a} . We observe in Fig. 3 that at $V_{\text{GS}} = 40$ V, E_{act} saturates at 15 meV, which is very close to $E_{\text{a}} = 11$ meV. This shows that our DOS parameters extracted from multi-frequency C - V spectroscopy are reliable.

Based on our experimental data and the extracted parameters, we construct a model for the subgap DOS of a-IGZO, which is shown in Fig. 4. As previously mentioned, the conduction band tail and deep-gap states are given by exponential and Gaussian distributions with parameters extracted from multi-frequency C - V measurements. We can combine (2) and (3) into a single expression

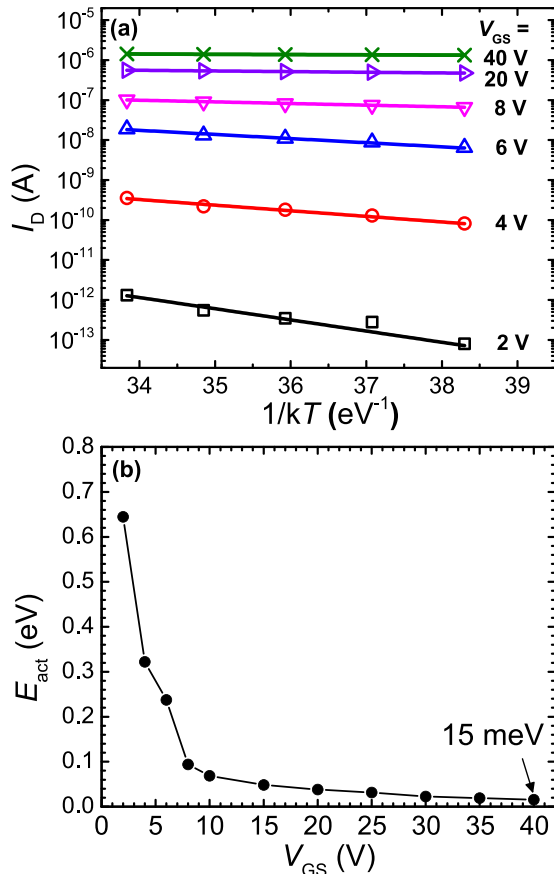


FIG. 3. (a) The Arrhenius plot used to extract the a-IGZO activation energy E_{act} from the temperature-dependent TFT I - V characteristics from 30 °C to 70 °C. (b) The activation energy of a-IGZO as a function of TFT gate-source voltage. The activation energy saturates at $E_{\text{act}} = 15$ meV for high gate biases.

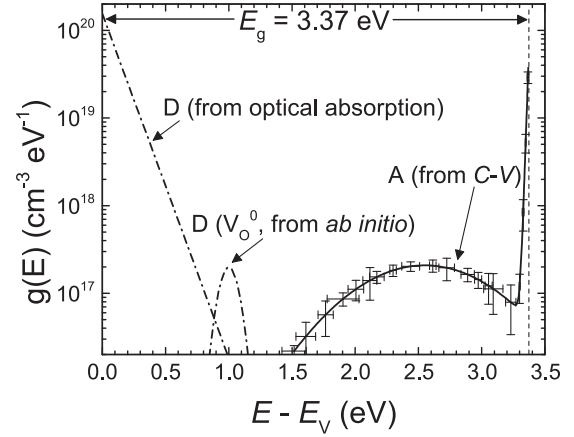


FIG. 4. The proposed a-IGZO subgap DOS model derived for electrical and optical characterization. The fully occupied deep-gap donor states (V_{O}^0) are adopted from first-principles calculations in the literature.⁷

$$g_{\text{a}}(E) = g_{\text{ta}}(E) + g_{\text{ga}}(E) = N_{\text{ta}} \exp\left(\frac{E - E_{\text{C}}}{E_{\text{a}}}\right) + N_{\text{ga}} \exp\left[-\frac{(E - \lambda_{\text{a}})^2}{\sigma_{\text{a}}^2}\right]. \quad (4)$$

The above equation alone provides no information about the donor/acceptor assignment of the g_{ga} states. In semiconductors, donor-like defect states are charge-neutral when occupied by electrons and positively charged when empty, whereas acceptors are charge-neutral when empty and negatively charged when occupied by electrons.²³ Most states above the Fermi level are assumed to be occupied by electrons, and empty for below. The multi-frequency C - V method for extracting the DOS is responsive to both trapping and de-trapping of charge carriers at defect states and cannot differentiate between the two processes. Two-dimensional numerical simulations have shown that donor assignment has no impact on TFT threshold voltage (V_{th}), while acceptor assignment causes V_{th} to shift with peak density. The latter is consistent with experimental TFT I - V characteristics, therefore we designate the conduction band deep-gap states to be acceptor-like as shown in the figure. Although this assignment is different from what was used in previous work on a-IGZO TFT numerical simulations,²⁰ it best describes the data collected in this study.

For the density of subgap states near the E_{V} , we also represent the valence bandtail states using an exponential expression

$$g_{\text{td}}(E) = N_{\text{td}} \exp\left(\frac{E_{\text{V}} - E}{E_{\text{d}}}\right), \quad (5)$$

where N_{td} is the maximum density of the valence band tail states and E_{d} is the valence bandtail slope. From the results of our optical absorption experiment and the TPC spectrum in the literature, we have extracted the Urbach energy to be $E_{\text{O}} = 110$ meV. Though the Urbach edge is given by the convolution of the conduction and valence bandtail states, the characteristic energy width of the conduction bandtail states is much smaller than the Urbach energy. Therefore, we expect the valence bandtail states to dominate the joint DOS

of a-IGZO, similar to a-Si:H¹, which allows us to approximate the slope of the Urbach edge as the valence bandtail slope ($E_d \approx E_0 = 110$ meV). In our model, we have adopted $N_{td} = 1.5 \times 10^{20} \text{ cm}^{-3} \text{ eV}^{-1}$ from the literature.²⁰

From first-principles calculations based on density functional theory, it was found that oxygen vacancies form fully occupied deep donor levels (V_O^0) in both crystalline⁷ and amorphous⁵ IGZO located around 1.0 eV above E_V . The large molecular spacing of the oxygen vacancy is expected to trap and prevent the electrons from being released. We adopt this in our model in the form of a Gaussian distribution

$$g_{gd}(E) = N_{gd} \exp \left[-\frac{(E - \lambda_d)^2}{\sigma_d^2} \right], \quad (6)$$

where $N_{gd} = 2 \times 10^{17} \text{ eV}^{-1} \text{ cm}^{-3}$, $\lambda_d = 1.0$ eV, and $\sigma_d = 0.1$ eV. Similar to the conduction band subgap states, the valence band tail and deep-gap states can also be combined into a single expression

$$g_d(E) = g_{td}(E) + g_{gd}(E) \\ = N_{td} \exp \left(\frac{E_V - E}{E_d} \right) + N_{gd} \exp \left[-\frac{(E - \lambda_d)^2}{\sigma_d^2} \right]. \quad (7)$$

The parameters of our a-IGZO DOS model are summarized in Table I.

Our DOS model can be used to explain the PL emission spectrum described earlier in Fig. 1(b). In the case of trap-to-trap transition, the recombination energy is only 1.5 eV, which is much lower than 2.76 eV and therefore cannot be responsible for the deep-level emission we have observed. The remaining two scenarios of band-to-hole trap (transition energy 2.37 eV) and electron trap-to-band (transition energy 2.55 eV) are potential candidates. In the former, the oxygen vacancy deep donor could trap a hole and then hypothetically recombine with a photo-excited electron in the conduction band. Although oxygen vacancy defects are often cited as the source of deep-level green emission in ZnO,²⁴ Taniguchi *et al.*¹⁴ and colleagues have shown experimentally that they may act as non-radiative recombination centers in a-IGZO. The intensity of deep-level emissions is quenched for a-IGZO deposited in low oxygen partial pressure¹³ (P_{O_2}) or annealed in oxygen-deficient ambient¹⁴ (i.e., N_2), both of which are assumed to enhance the formation of oxygen vacancies. This would eliminate all but the electron trap-to-band transition as the origin of the deep-level emission. Regarding the nature of the electron trap states, Ide *et al.*

suggested that excess/weakly bonded oxygen in the a-IGZO microstructure can exist as a broad distribution of deep-gap states near E_C .²⁵ Desorption of O_2 was observed in thermal desorption spectrum measurements for a-IGZO films annealed in O_3 or O_2 ambient or deposited under high oxygen partial pressure (P_{O_2}). Results from our group²⁶ and in the literature²⁷ also indicate that P_{O_2} has a strong impact on g_{ga} . This is consistent with our assignment based on numerical simulations that g_{ga} are acceptor-like because excess/weakly bonded oxygen can accept/capture electron through $O^0 + e^- \rightarrow O^{1-}$ and/or $O^{1-} + e^- \rightarrow O^{2-}$. The O^{2-} ion cannot capture any electrons because of its filled outer shell. In this physical picture, the photo-excited electron falls to the band edge and then to an electron trap through scattering. It then radiatively recombines with a hole in the valence band, emitting at energy of 2.55 eV. The fact that the shape of the deep-level emission and the g_{ga} deep-gap states are very similar also supports this proposition.

It is informative to compare the DOS of a-IGZO with that of a-Si:H, which also consists of exponential tail states and Gaussian deep-gap states.^{1,2} In a-Si:H, the conduction and valence band tail states are a result of fluctuations of the Si-Si bond angles and lengths. Structural disorder also causes the bandtail states in a-IGZO, but its conduction band tail slope is sharper and the peak density is at least one to two orders of magnitude lower than a-Si:H because of the large overlapping s orbitals of the heavy In^{3+} cation.²⁸ The deep-gap states in a-Si:H are mainly attributed to dangling Si bonds and can be greatly reduced by optimized hydrogenation. The deep-gap states for a-IGZO, due to its nature as an oxide semiconductor, can be attributed to localized oxygen-deficiency or excess oxygen in the a-IGZO thin film. As mentioned in this work, oxygen vacancies and excess oxygen in the a-IGZO microstructure form deep donor states and deep acceptor states, respectively. Kamiya and Hosono stated that low P_{O_2} during deposition produces films with high electron density and this is linked to oxygen vacancies, whereas the low electron density in high P_{O_2} -deposited films is attributed to excess oxygen.²⁹ We note that the impact of P_{O_2} on carrier density can be described using only oxygen vacancies, or only excess oxygen, or both. Both descriptions are consistent with our conclusion that the transition from g_{ga} to E_V is responsible for the deep-level PL emission.

IV. CONCLUSION

We have developed a comprehensive and robust subgap DOS model for a-IGZO based on a combination of experimental results and information available in the literature. The valence bandtail states are defined by parameters extracted from optical absorption and TPC spectroscopy. We adopt the results of first-principles calculations of a-IGZO in the literature, which states that oxygen vacancies form fully occupied deep donor states near the valence band. The conduction band tail and deep-gap states are extracted by multi-frequency $C-V$ spectroscopy. Numerical simulations indicate that the conduction band deep-gap states originate from excess oxygen acting as electron acceptors. Recombination of an electron trapped in the

TABLE I. Parameters used in the proposed a-IGZO subgap DOS model.

Conduction band subgap states				
$N_{ta} (\text{cm}^{-3} \text{ eV}^{-1})$	$E_a (\text{meV})$	$N_{ga} (\text{cm}^{-3} \text{ eV}^{-1})$	$\lambda_a (\text{eV})$	$\sigma_a (\text{eV})$
4.23×10^{19}	11 ± 0.3	2.08×10^{17}	2.55 ± 0.37	0.69
Valence band subgap states				
$N_{td} (\text{cm}^{-3} \text{ eV}^{-1})$	$E_d (\text{meV})$	$N_{gd} (\text{cm}^{-3} \text{ eV}^{-1})$	$\lambda_d (\text{eV})$	$\sigma_d (\text{eV})$
1.55×10^{20}	110	2.0×10^{17}	1.0	0.01

conduction band deep-gap state and a hole in the valence band is responsible for the deep-level emission in the PL spectrum of a-IGZO thin film. We have used this DOS model in 2D numerical simulations to obtain electrical properties of a-IGZO metal-semiconductor field-effect transistors in good agreement with experimental data, and the results are published elsewhere.³⁰

ACKNOWLEDGMENTS

D. H. Kim acknowledges financial supports from the LG Yonam Foundation and the BK21+ with the Educational Research Team for Creative Engineers on Material-Device-Circuit Co-Design (Grant No. 22A20130000042). The authors would like to thank Dr. T.-C. Fung for conducting the PL spectroscopy experiments on the a-IGZO thin film. E. K.-H. Yu would like to thank K.-C. Cheng for conducting numerical analysis on the optical absorption spectrum.

- ¹R. A. Street, *Hydrogenated Amorphous Silicon* (Cambridge University Press, 2005).
- ²J. Kanicki and S. Martin, "Hydrogenated amorphous silicon thin-film transistors," in *Thin-Film Transistors*, edited by C. R. Kagan and P. Andry (CRC Press, 2003), pp. 71–137.
- ³H.-H. Hsieh, T. Kamiya, K. Nomura, H. Hosono, and C.-C. Wu, *Appl. Phys. Lett.* **92**, 133503 (2008).
- ⁴K. Nomura, T. Kamiya, H. Yanagi, E. Ikenaga, K. Yang, K. Kobayashi, M. Hirano, and H. Hosono, *Appl. Phys. Lett.* **92**, 202117 (2008).
- ⁵T. Kamiya, K. Nomura, M. Hirano, and H. Hosono, *Phys. Status Solidi C* **5**, 3098 (2008).
- ⁶T. Fung, C. Chuang, K. Nomura, H. D. Shieh, H. Hosono, and J. Kanicki, *J. Inf. Disp.* **9**, 21 (2008).
- ⁷C. Chen, K.-C. Cheng, E. Chagarov, and J. Kanicki, *Jpn. J. Appl. Phys., Part 1* **50**, 091102 (2011).
- ⁸C. Chen, K. Abe, H. Kumomi, and J. Kanicki, *IEEE Trans. Electron Devices* **56**, 1177 (2009).
- ⁹S. Lee and A. Nathan, *Appl. Phys. Lett.* **101**, 113502 (2012).
- ¹⁰M. Kimura, T. Nakanishi, K. Nomura, T. Kamiya, and H. Hosono, *Appl. Phys. Lett.* **92**, 133512 (2008).
- ¹¹K. Jeon, C. Kim, I. Song, J. Park, S. Kim, S. Kim, Y. Park, J.-H. Park, S. Lee, D. M. Kim, and D. H. Kim, *Appl. Phys. Lett.* **93**, 182102 (2008).
- ¹²S. Lee, S. Park, S. Kim, Y. Jeon, K. Jeon, J.-H. Park, J. Park, I. Song, C.-J. Kim, Y. Park, D. M. Kim, and D. H. Kim, *IEEE Electron Device Lett.* **31**, 231 (2010).
- ¹³N. Yamaguchi, S. Taniguchi, T. Miyajima, and M. Ikeda, *J. Vac. Sci. Technol., B* **27**, 1746 (2009).
- ¹⁴S. Taniguchi, N. Yamaguchi, T. Miyajima, and M. Ikeda, "Optical and electrical characteristics of amorphous InGaZnO after annealing," (MRS Symp. Proc., 2008).
- ¹⁵N. Ishihara, M. Tsubuku, Y. Nonaka, R. Watanabe, K. Inoue, H. Shishido, K. Kato, and S. Yamazaki, in *2012 19th International Workshop on Active-Matrix Flatpanel Displays and Devices AM-FPD* (2012), pp. 143–146.
- ¹⁶F. Urbach, *Phys. Rev.* **92**, 1324 (1953).
- ¹⁷P. T. Erslev, Ph.D. Thesis, University of Oregon, 2010.
- ¹⁸A. V. Gelatos, J. D. Cohen, and J. P. Harbison, *Appl. Phys. Lett.* **49**, 722 (1986).
- ¹⁹J. D. Cohen, J. T. Heath, and W. N. Shafarman, in *Wide-Gap Chalcopyrites*, edited by S. Siebentritt and U. Rau (Springer, Berlin Heidelberg, 2006), pp. 69–90.
- ²⁰T.-C. Fung, C.-S. Chuang, C. Chen, K. Abe, R. Cottle, M. Townsend, H. Kumomi, and J. Kanicki, *J. Appl. Phys.* **106**, 084511 (2009).
- ²¹K. Nomura, T. Kamiya, H. Ohta, K. Shimizu, M. Hirano, and H. Hosono, *Phys. Status Solidi A* **205**, 1910 (2008).
- ²²C. Chen and J. Kanicki, "Influence of the density of states and series resistance on the field-effect activation energy in a-Si:H TFT," (MRS Symp. Proc., 1996), p. 77.
- ²³S. M. Sze and K. K. Ng, *Physics of Semiconductor Devices* (John Wiley & Sons, 2006).
- ²⁴K. Vanheusden, W. L. Warren, C. H. Seager, D. R. Tallant, J. A. Voigt, and B. E. Gnade, *J. Appl. Phys.* **79**, 7983 (1996).
- ²⁵K. Ide, Y. Kikuchi, K. Nomura, M. Kimura, T. Kamiya, and H. Hosono, *Appl. Phys. Lett.* **99**, 093507 (2011).
- ²⁶Y.-S. Lee, E. K.-H. Yu, D.-H. Shim, H.-S. Kong, L. Bie, and J. Kanicki, "Oxygen flow effects on electrical properties, stability, and density of states of amorphous In-Ga-Zn-O thin-film transistors" (unpublished).
- ²⁷S. Kim, Y. W. Jeon, Y. Kim, D. Kong, H.-K. Jung, M.-K. Bae, J.-H. Lee, B. D. Ahn, S. Y. Park, J.-H. Park, J. Park, H.-I. Kwon, D. M. Kim, and D. H. Kim, *IEEE Electron Device Lett.* **33**, 62 (2012).
- ²⁸T. Kamiya, K. Nomura, and H. Hosono, *J. Disp. Technol.* **5**, 468 (2009).
- ²⁹T. Kamiya and H. Hosono, *ECS Trans.* **54**, 103 (2013).
- ³⁰C. Zhao, L. Bie, R. Zhang, and J. Kanicki, *IEEE Electron Device Lett.* **35**, 75 (2014).